Supporting Information

Architecture Designed ZnO Hollow Microspheres with Wide-range Visible-light Photoresponses

Ziqi Sun[§], Ting Liao[¶], Jae-Geun Kim[§], Kesong Liu[†,], Lei Jiang[†,‡], Jung Ho Kim[§,*], Shi Xue Dou[§]*

[§]Institute for Superconducting and Electronic Materials, University of Wollongong, Innovation Campus, North Wollongong, NSW 2500, Australia

[¶]Australian Institute for Bioengineering and Nanotechnology, the University of Queensland, St Lucia, QLD 4072, Australia

[†]Key Laboratory of Bio-inspired Smart Interfacial Science and Technology of Ministry of Education, School of Chemistry and Environment, Beihang University, Beijing 100191, China

[‡]Beijing National Laboratory for Molecular Sciences (BNLMS), Key Laboratory of Organic Solids, Institute of Chemistry, Chinese Academy of Sciences, Beijing 100190, China

* jhk@uow.edu.au, liuks@buaa.edu.cn

Experimental Procedures

1.1 Materials

The chemical reagents used for the synthesis of ZnO hollow microspheres with designed architectures are commercially available reagents. Zinc acetate dihydrate ($ZnAc_2 \cdot 2H_2O$, 99.5%), polyethylene oxide - polypropylene oxide - polyethylene oxide (PEO_{20}-PPO_{70}-PEO_{20}, Pluronic P123, M_n = 5,800), ethylene glycol (EG, 99.8%), absolute ethanol (EtOH), and hexamethylenetetramine (HMTA, 99.0%) were purchased from Sigma-Aldrich. All the chemicals were used as received without further purification.

1.2 Synthesis of ZnO hollow microspheres

1.2.1 Synthesis of ZnO hollow microspheres with solid smooth surface

In a typical experimental procedure, 0.2 g Pluronic P123 was added into 3 g EtOH, and together with 0.44 g H_2O and 0.2 g $ZnAc_2 \cdot 2H_2O$, or 0.41 g H_2O and 0.4 g $ZnAc_2 \cdot 2H_2O$, then 0.25 g or 0.09 g HMTA, respectively, was added under stirring, and then 46 ml EG was put into the ethanol solution. After stirring for 10 min, a transparent solution was obtained. The

transparent precursor solution was divided into two parts, transferred into two 45 ml autoclaves, and heated at 110 ^{o}C for 15 h. The products of the solvothermal reaction were washed with distilled water and ethanol 3 times, and the light yellow powders were collected after washing/centrifugation and drying at 80 ^{o}C for 24 h. Some powders were redispersed in ethanol by ultrasonication for further characterization.

1.2.2 Synthesis of ZnO hollow microspheres with nanowire network building units

0.2 g Pluronic P123 was added into 3 g EtOH with 0.44 g water and stirred for 15 min to form a clear solution, and then 0.2 g $ZnAc_2 \cdot 2H_2O$ and 0.09 g HMTA were added into the surfactant solution. After stirring for around 15 min, a clear solution was obtained. Then, 46 ml EG was put into the ethanol solution. After stirring for 30 min, a transparent solution was obtained. The obtained EtOH + EG precursor solution was statically aged for 3 days. After aging, the transparent precursor solution was divided into two parts, transferred into two 45 ml autoclaves, and heated at 110 ^{o}C for 15 h. The products of the solvothermal reaction were washed with distilled water and ethanol 3 times, and the light yellow powders were collected after washing/centrifugation and drying at 80 ^{o}C for 24 h. Some powders were redispersed in water and ethanol by ultrasonication for further characterization.

1.2.3 Synthesis of ZnO hollow microspheres with nanosheet stack building units

0.2 g Pluronic P123 was added into 3 g EtOH with 0.45 g H_2O to form a clear solution with stirring for 15 min, and then 0.1 g $ZnAc_2 \cdot 2H_2O$ and 0.045 g HMTA were added into the ethanol solution. After stirring for around 15 min, a clear solution was obtained. Then, 46 ml EG was put into the ethanol solution. After stirring for 30 min, a transparent solution was obtained. The obtained EtOH + EG precursor solution was statically aged for 3 days or 7 days. After aging, the transparent precursor solution was divided into two parts, transferred into two 45 ml autoclaves, and heated at 110 ^{o}C for 15 h. The products of the solvothermal reaction were washed with distilled water and ethanol 3 times, and the light yellow powders were

collected after washing/centrifugation and drying at 80 ^{o}C for 24 h. Some powders were redispersed in water and ethanol by ultrasonication for further characterization.

1.2.4 Two-Step Synthesis of ZnO hollow microspheres with mesoporous nanoball constituent units

0.2 g Pluronic P123 was added into 3 g EtOH with the desired amount of water (0.44 g H_2O for 0.2 g $ZnAc_2 \cdot 2H_2O$, or 0.41 g H_2O for 0.4 g $ZnAc_2 \cdot 2H_2O$) and stirred for 15 min to form a clear solution, and then 0.2 g $ZnAc_2 \cdot 2H_2O$ and 0.25 g HMTA, or 0.4 g $ZnAc_2 \cdot 2H_2O$ and 0.09 g HMTA were added into the surfactant solution. After stirring for around 15 min, a clear solution was obtained. Then, 46 ml EG was put into the ethanol solution. After stirring for 30 min, a transparent solution was obtained. The obtained EtOH + EG precursor solution was statically aged for 7 days. After aging, the transparent precursor solution was divided into two parts, transferred into two 45 ml autoclaves, and heated at 110 ^{o}C for 15 h. The products of the solvothermal reaction were washed with distilled water and ethanol 3 times, and the light yellow powders were collected after washing/centrifugation and drying at 80 ^{o}C for 24 h. Some powders were redispersed in water and ethanol by ultrasonication for further characterization.

1.3 Characterizations

The composition and phase of the as-prepared products were measured by a powder X-ray diffractometer (XRD, MMA, GBC Scientific Equipment LLC, Hampshire, IL, USA) with Cu K_{α} radiation. The morphology of the samples was observed with a scanning electron microscope (SEM, JSM-7500FA, JEOL, Tokyo, Japan). High resolution transmission electron microscope observation was carried out using a JEM-2011F (HRTEM, JEOL, Tokyo, Japan) operated at 200 kV. Surface area was measured by a surface area analyzer (NOVA1000, Quantachrome Co., FL, USA) at 77 K. Before measurement, the sample was heated at 120 ^{o}C for 5 h. The specific surface area was calculated based on the slop and intercept of the linear

adsorption isotherm in the p/p0 range over 0.05 to 0.35, according to the BET theory. For each sample, three batches of powders were measured for average. Ultraviolet-Visible (UV-Vis) absorption spectra were collected on the thin films of ZnO hollow microspheres, which prepared by spin coating 10 wt.% aqueous ZnO hollow microsphere suspensions on transparent glasses and followed with heating at 400 ^{o}C for 1 h to remove the influence of residual surfactant molecules, on a UV-Visible light absorption spectroscope in the wavelength range of 195-800 nm (Shimadzu UV-3600, Japan).

For the photoresponse testing, the ZnO hollow microsphere thin films were prepared by spin coating 10 Wt% aqueous suspensions at 2000 rpm for 5 times on a FTO glass and then heated at 400 ^{o}C for 2 h. Thin films with an active area of 1 cm^2 were assembled with a FTO counter electrode. Photocurrent of the thin films was examined by a Keithley 2400 source meter under alternative visible-light (λ > 420 nm, 65 $mW \cdot cm^{-2}$) and dark illumination at 1 V bias and 10 s or 30 s intervals. In some cases, the alternating simulated solar light (100 $mW \cdot cm^{-2}$) and visible light illumination as well as the alternating pure UV irradiation (325 nm, 15 $mW \cdot cm^{-2}$) and dark with a 10 s interval were also employed for photocurrent measurements. The quantum emission efficiency of the nanostructures was tested under monochromatic irradiation between 300-800 nm on the samples that were assembled with a Pt counterelectrode and filled with a commercial electrolyte purchased from Solaronix (Iodolyte AN-50) to promote the electron transport between the electrodes. The utilization of electrolyte may slightly influence the visible light responses around 550 nm, but it seems essential to obtain distinguishable signals.

Table S1: Compositions of precursor solutions and aging time and the ZnO hollow microspheres after synthesis.

Sample numbers	Composition of reaction solution	Aging time	Morphology of hollow spheres	Shape of constituent units	Average size
ZSH-1	2P123:4.1H_2O:30EtOH:4ZnAc_2·2H_2O:2.5HMTA:500EG	0	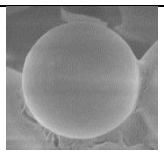	Solid shell	2.27±0.46 μm
ZSH-1'	2P123:4.4H_2O:30EtOH:2ZnAc_2·2H_2O:0.9HMTA:500EG	0			3.57±0.49 μm
ZSH-2	2P123:4.4H_2O:30EtOH:2ZnAc_2·2H_2O:0.9HMTA:500EG	3 days	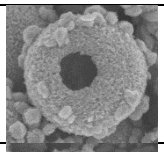	1D nanowire network	2.00±0.19 μm
ZSH-3	2P123:4.5H_2O:30EtOH:1ZnAc_2·2H_2O:0.45HMTA:500EG	3 days	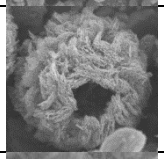	2D nanosheet stack	1.50±0.18 μm
ZSH-3'	2P123:4.5H_2O:30EtOH:1ZnAc_2·2H_2O:0.45HMTA:500EG	7 days	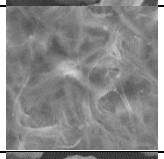	2D nanosheet	N/A
ZSH-4	2P123:4.4H_2O:30EtOH:2ZnAc_2·2H_2O:0.9HMTA:500EG	7 days	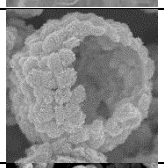	3D nanoball block	1.03±0.16 μm
ZSH-4'	2P123:4.1H_2O:30EtOH:4ZnAc_2·2H_2O:2.5HMTA:500EG	7 days	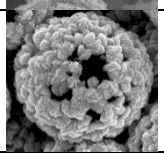	3D nanoball block	1.78±0.25 μm

Figure S1

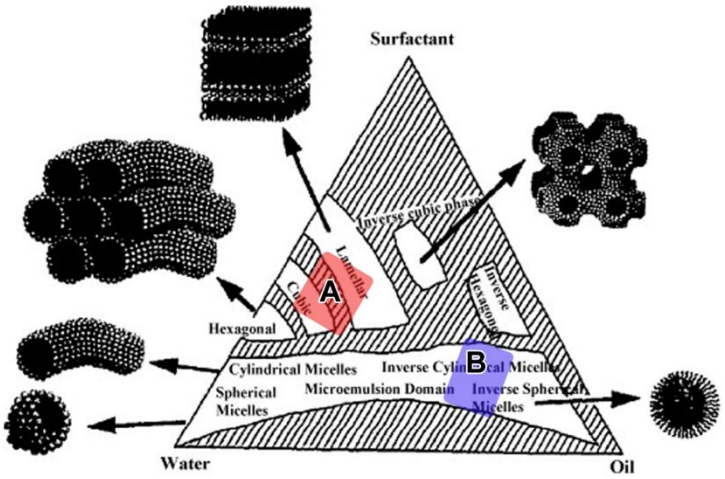

Figure S1: Schematic phase diagram of surfactant-water-oil systems showing a variety of self-assembled structures The area "A" in (a) indicates the desired starting proportion of surfactant-water-oil to form expected nanostructured building constituents, and area "B" indicates the desired proportion of surfactant-water-oil during hydrothermal and with the addition of EG to form shelled spherical structures. (Adapted from J. Liu *et al, Adv. Colloid. Inter. Sci.* 1996, **69**, 131.)

Figure S2

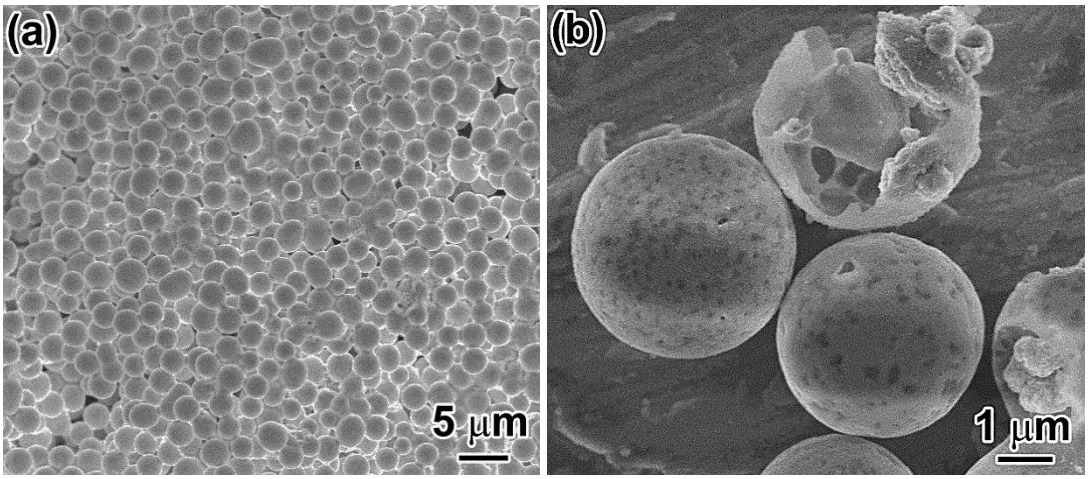

Figure S2: (a) Low-magnification and (b) high-magnification images of ZnO hollow microspheres synthesized from the 2P123:4.4H_2O:30EtOH:2$ZnAc_2 \cdot 2H_2O$:0.9HMTA:500EG solution without aging (ZHS-1').

Figure S3

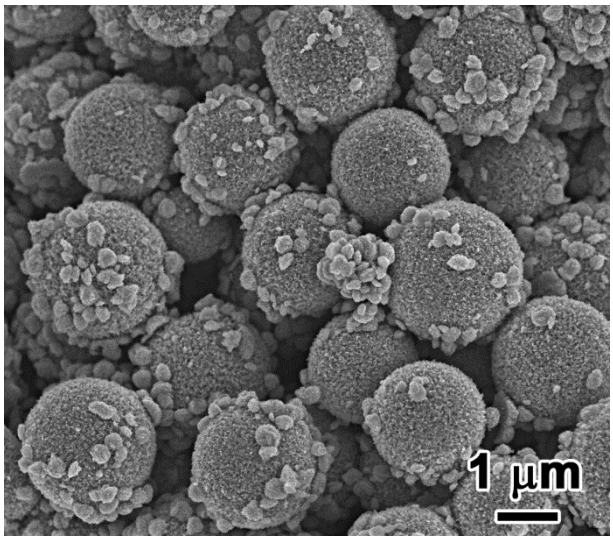

Figure S3: Low magnification image of ZnO hollow microspheres synthesized from the 2P123:4.4H_2O:30EtOH:2$ZnAc_2$·2H_2O:0.9HMTA:500EG solution and aged for 3 days (ZHS-2.

Figure S4

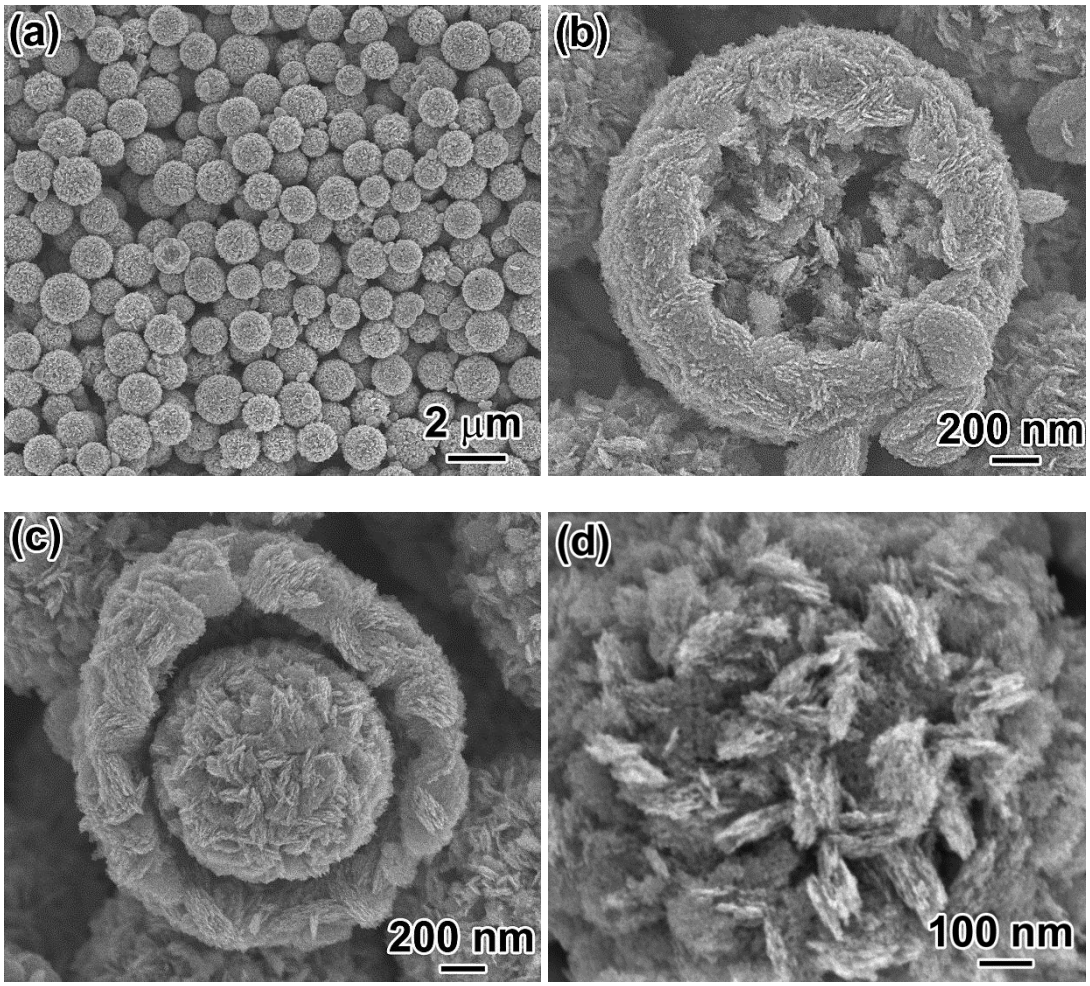

Figure S4: (a) Low magnification image of hollow microspheres synthesized from the 2P123:4.5H_2O:30EtOH:1ZnAc_2·2H_2O:0.45HMTA:500EG solution and aged for 3 days (ZHS-3); (b) high magnification image of a half microsphere; (c) high magnification image of a double layered hollow microsphere; and (d) high magnification image of the constituent nanosheet stacks.

Figure S5

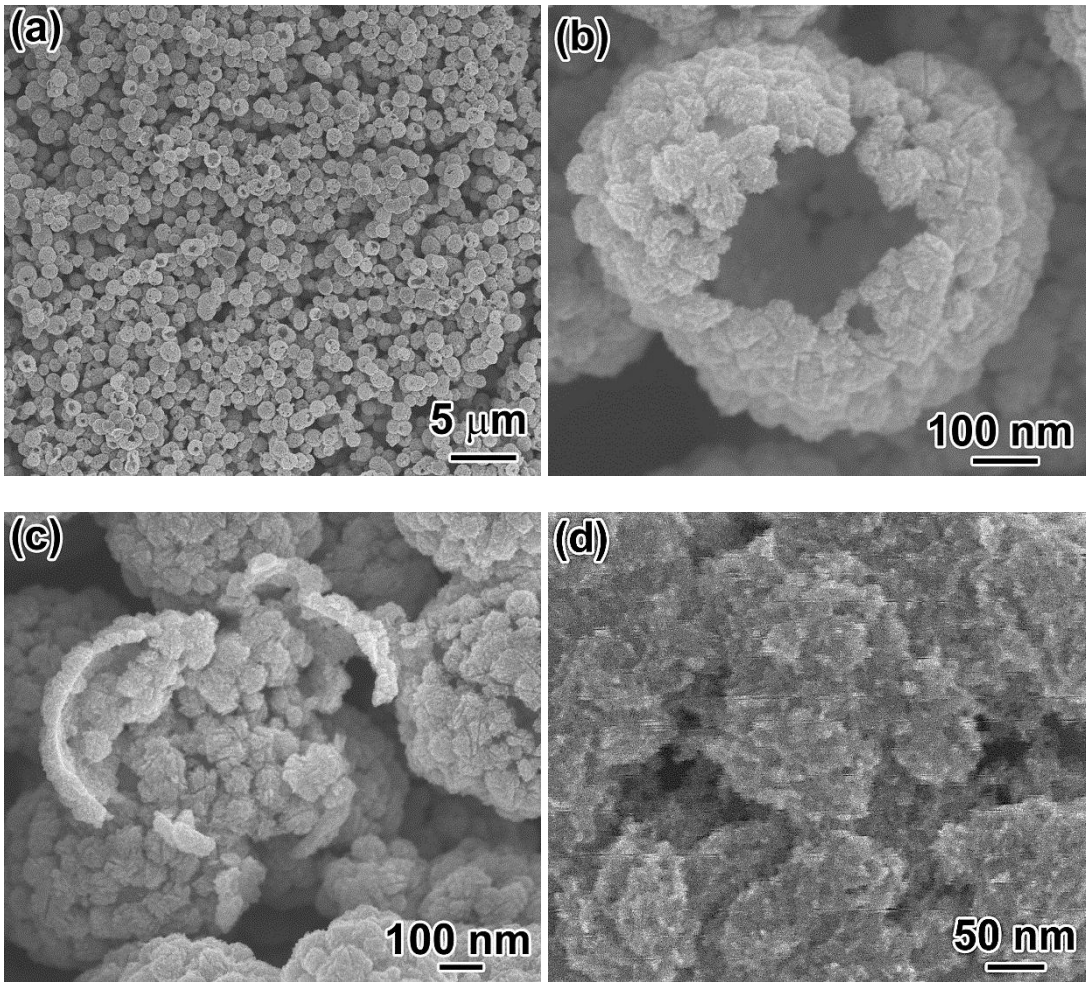

Figure S5: (a) Low magnification and (b) high magnification SEM images of ZnO microspheres composed of nanoball blocks that were synthesized from the 2P123:4.4H_2O:30EtOH:2$ZnAc_2$·2H_2O:0.9HMTA:500EG solution and aged for 7 days (ZHS-4); (c) high magnification SEM image of one broken ZHS-4 hollow microspheres with a well-defined shell structure; and (d) high magnification image of the building blocks of ZHS-4.

Figure S6

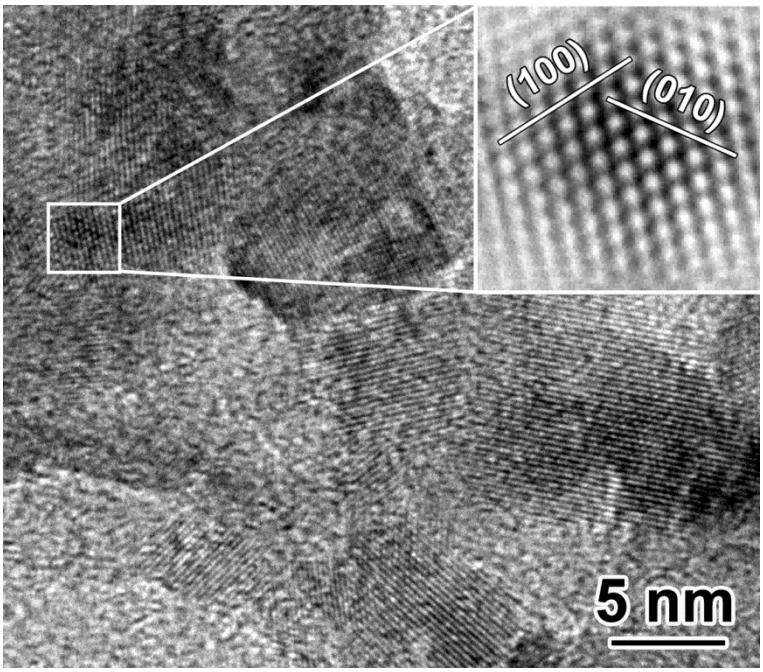

Figure S6: HRTEM image of the nanowires in the shells of the hollow microspheres of ZSH-2.

Figure S7

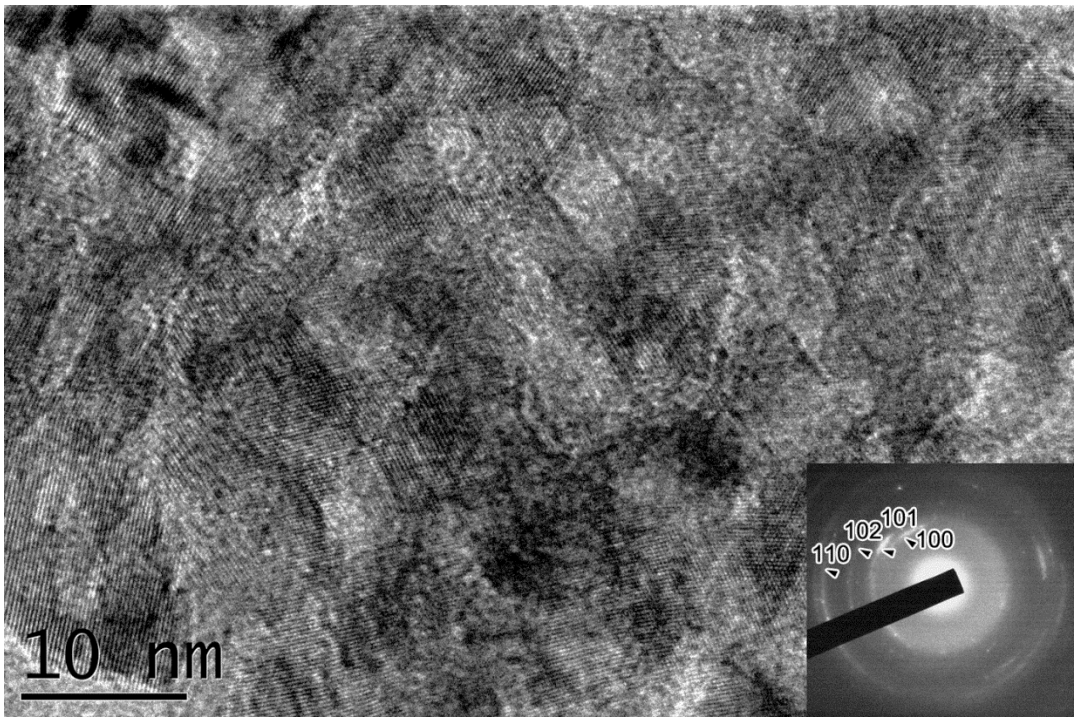

Figure S7: HRTEM image of the nanosheets in the shells of the hollow microspheres of ZSH-3. The inset is the corresponding selected area electron diffraction (SAED) pattern.

Figure S8

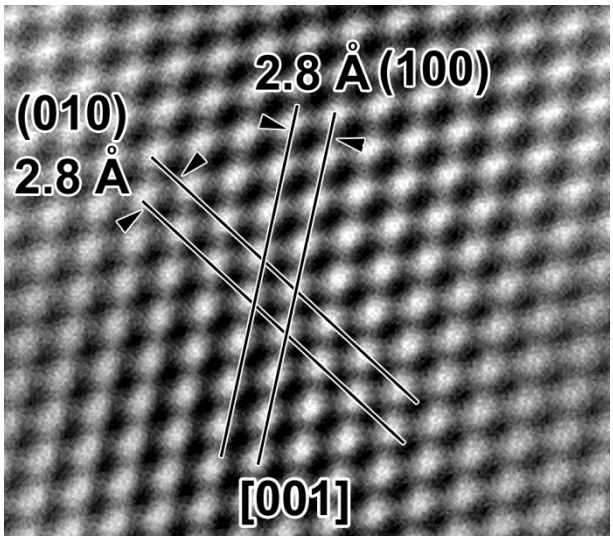

Figure S8: HRTEM image of the ZnO nanocrystallites in the constituent nanosheet stacks of ZSH-3.

Figure S9

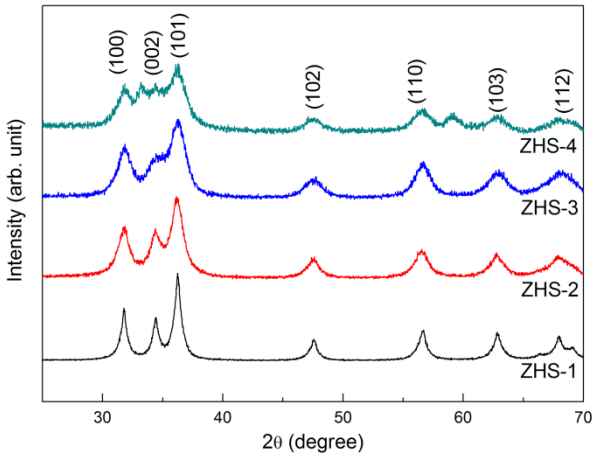

Figure S9: XRD patterns of ZnO hollow microspheres.

Figure S10

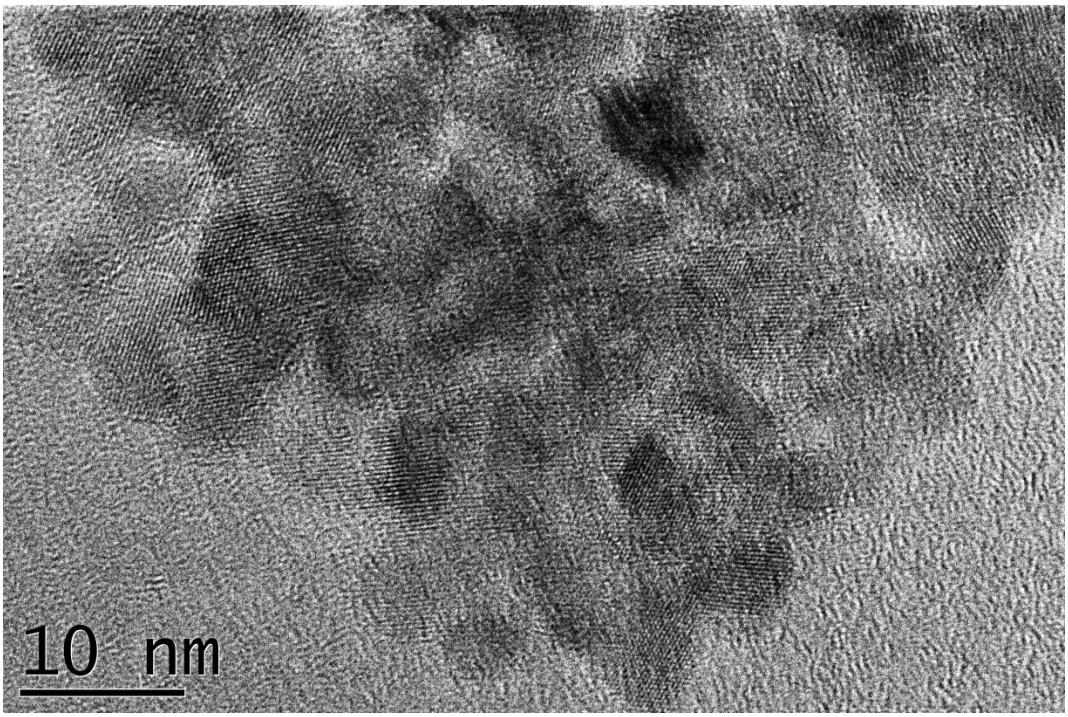

Figure S10: HRTEM image of the nanowires in the shells of the hollow microspheres of ZSH-4.

Figure S11

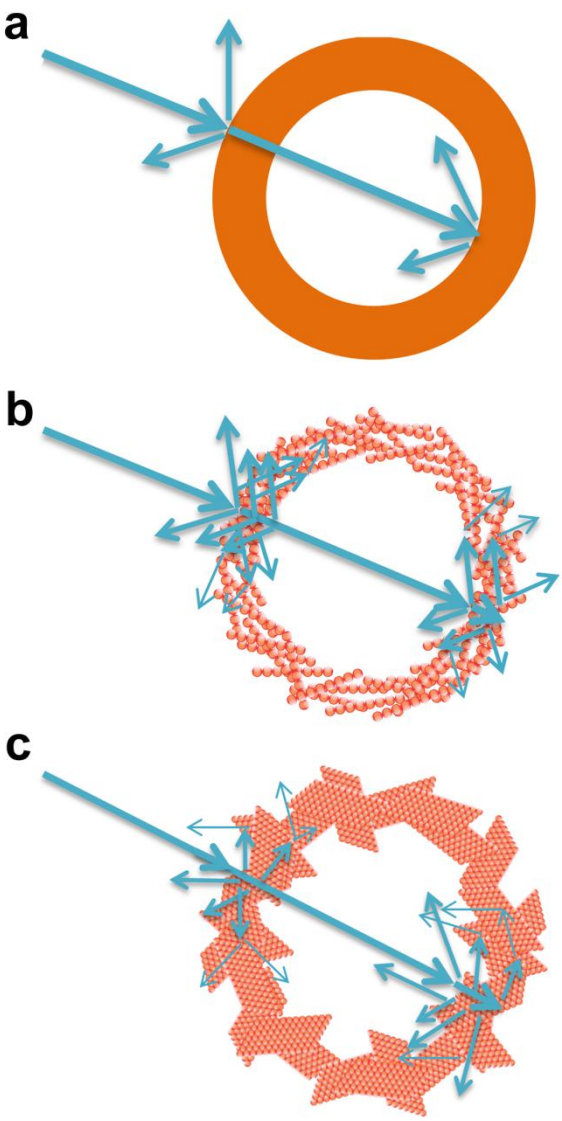

Figure S11: Schematic drawing that shows the multiple light reflections within ZnO hollow spheres with: (a) a solid shell, (b) a nanowire shell, and (c) a nanosheet shell.

Figure S12

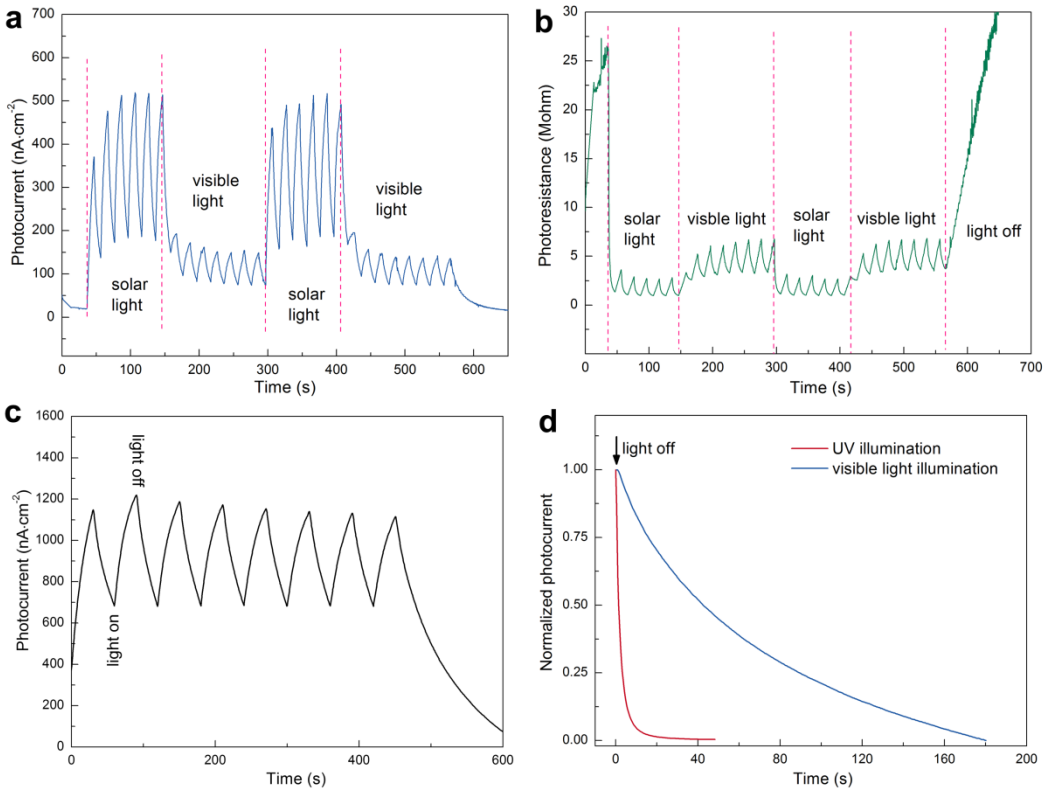

Figure S12: (a) Photoresponse behavior of ZHS-2 under alternating solar light and visible light illumination; (b) variation of resistance of photoelectrode of ZHS-2 under alternating soalr light and visible light illumination; (c) Visible-light photoresponses of ZnO hollow microsphere electrodes in the morphology of 3D mesoporous nanoballs (ZHS-4), under alternative visible-light and dark illumination at 1 V bias and 30 s interval; and (d) photocurrent decay behavior of ZHS-4 after UV-irradiation and visible light illumination, respectively.